International Journal of Nanomedicine

Dovepress
open access to scientific and medical research

Open Access Full Text Article

ORIGINAL RESEARCH

Adiponectin-coated nanoparticles for enhanced imaging of atherosclerotic plaques

This article was published in the following Dove Press journal:
International Journal of Nanomedicine
20 June 2011
Number of times this article has been viewed

Gunter Almer[1,6]
Karin Wernig[2]
Matthias Saba-Lepek[3]
Samih Haj-Yahya[1]
Johannes Rattenberger[4]
Julian Wagner[4]
Kerstin Gradauer[3]
Daniela Frascione[3]
Georg Pabst[3]
Gerd Leitinger[5]
Harald Mangge[1]
Andreas Zimmer[2]
Ruth Prassl[3]

[1]Clinical Institute of Medical and Chemical Laboratory Diagnostics, [2]Institute of Pharmaceutical Sciences, Department of Pharmaceutical Technology, University of Graz, [3]Institute of Biophysics and Nanosystems Research, Austrian Academy of Science, [4]Institute for Electron Microscopy and Fine Structure Research, Graz University of Technology, [5]Institute of Cell Biology, Histology and Embryology, Medical University of Graz, [6]Center for Medical Research, Medical University of Graz, Austria

Background: Atherosclerosis is a leading cause of mortality in the Western world, and plaque diagnosis is still a challenge in cardiovascular medicine. The main focus of this study was to make atherosclerotic plaques visible using targeted nanoparticles for improved imaging. Today various biomarkers are known to be involved in the pathophysiologic scenario of atherosclerotic plaques. One promising new candidate is the globular domain of the adipocytokine adiponectin (gAd), which was used as a targeting sequence in this study.

Methods: gAd was coupled to two different types of nanoparticles, namely protamine-oligonucleotide nanoparticles, known as proticles, and sterically stabilized liposomes. Both gAd-targeted nanoparticles were investigated for their potency to characterize critical scenarios within early and advanced atherosclerotic plaque lesions using an atherosclerotic mouse model. Aortic tissue from wild type and apolipoprotein E-deficient mice, both fed a high-fat diet, were stained with either fluorescent-labeled gAd or gAd-coupled nanoparticles. Ex vivo imaging was performed using confocal laser scanning microscopy.

Results: gAd-targeted sterically stabilized liposomes generated a strong signal by accumulating at the surface of atherosclerotic plaques, while gAd-targeted proticles became internalized and showed more spotted plaque staining.

Conclusion: Our results offer a promising perspective for enhanced in vivo imaging using gAd-targeted nanoparticles. By means of nanoparticles, a higher payload of signal emitting molecules could be transported to atherosclerotic plaques. Additionally, the opportunity is opened up to visualize different regions in the plaque scenario, depending on the nature of the nanoparticle used.

Keywords: adiponectin, nanoparticles, proticles, liposomes, molecular imaging, atherosclerosis

Introduction

In recent years it has become evident that adipose tissue performs various active metabolic and endocrine functions by delivering proactive cytokines, known as adipocytokines.[1,2] Among these are free fatty acids, adipsin, leptin, resistin, plasminogen activator inhibitor-1, tumor necrosis factor-α (TNF-α), and adiponectin.[3] Adiponectin consists of 247 amino acids, and is secreted specifically from differentiated adipocytes. The primary sequence of adiponectin, a 30 kDa polypeptide, consists of a signal sequence followed by a nonconserved N-terminal domain, 22 collagen repeats, and a C-terminal globular domain (gAd) which is structurally related to TNF-α.[4] In circulating blood, adiponectin appears at concentrations of 2–30 μg/mL,[2] and is subjected either to collagen-induced formation of trimers, hexamers, and higher oligomerized structures, or to rapid cleavage of the primary adiponectin sequence into

Correspondence: Ruth Prassl
Institute of Biophysics and Nanosystems Research, Austrian Academy of Sciences, Schmiedlstrasse 6, A-8042 Graz-Messendorf, Austria
Tel +43 31 64120305
Email ruth.prassl@oeaw.ac.at

the collagen-like region and into gAd (17 kDa),[3–5] which is found at lower levels (about 1% of total adiponectin) in the circulation.[6] gAd has been shown to have potent metabolic effects, particularly in skeletal muscle.[5] Furthermore, it has been shown to increase insulin-stimulated glucose uptake and to boost β-oxidation of fatty acids.[7,8] Apart from these antidiabetic properties, gAd shows anti-inflammatory as well as anti-atherosclerotic effects.[5,9] The latter are also associated with the ability of adiponectin to stimulate production of nitric oxide by endothelial cells.[10] As is well-known, endothelial damage induced by proinflammatory cytokines, such as TNF-α, has a crucial role in the formation of atherosclerosis. Endothelial damage leads to adhesion and penetration of monocytes into the endothelium, followed by transformation of macrophages into dangerous foam cells.[2] In parallel, it has been shown that adiponectin treatment reduces the size of the area of atherosclerotic plaques throughout the intima or adventitia.[11] Moreover, local treatment with adiponectin leads to inhibition of mRNA expression of VCAM-1 and ICAM-1 in the abdominal aortic tissue of atherosclerotic rabbits.[11]

When considering diagnostic applications, it is important to note that adiponectin is detected only in injured but not in intact vascular walls.[12,13] In unpublished data, we showed that gAd binds even more efficiently than full-length adiponectin to atherosclerotic plaques. In the present study, we exploited this superior binding affinity of gAd to atherosclerotic lesions using gAd as a targeting sequence attached to two different classes of nanoparticles.

The first type of nanoparticles we examined were protamine-oligonucleotide nanoparticles, known as proticles. Proticles are biodegradable nanoparticles, which have been previously developed and characterized by our group for the delivery of various active compounds, including antisense oligonucleotides or small peptides.[14–17] Proticles can be formulated by directed self-assembly of anionic and cationic biopolymers in combination with protamine, a cationic 32 amino acid peptide used in depot insulin. These nanoparticles can be coated with drug targeting sequences in a second production step.[18] Proticles are nontoxic and show no immunostimulatory properties.[19]

The second type of nanoparticles we tested were sterically stabilized liposomes, which are frequently used as drug delivery systems and increasingly utilized for targeted imaging.[20–22] Liposomes have several advantages because they are easily formulated using a flexible set of lipid building blocks for assembly. In general, they show high biocompatibility, and polymer-grafted liposome preparations exhibit prolonged residence times in the circulation,[23,24] and are reported to be nonimmunogenic.[25,26]

Each nanoparticle can be loaded with many signal emitting molecules. Therefore, we expected to see a brighter signal within plaque areas compared with the signal, which is generated by fluorescence-labeled gAd (one dye molecule per protein). To test this hypothesis, we coupled gAd to the abovementioned colloidal nanocarriers. By confocal laser scanning microscopy, we monitored the ability of these gAd-targeted nanoparticles to recognize, bind, and accumulate in atherosclerotic plaques in the aortic tissue of apolipoprotein E-deficient mice. The enrichment of signal emitting groups in the plaques would be a prerequisite for efficient, noninvasive in vivo molecular imaging using gAd-targeted nanoparticles.

Materials and methods

Materials

Oligonucleotides, as well as Alexa-488-labeled oligonucleotides (Alexa-488-ON) were obtained from Biospring GmbH (Frankfurt, Germany). A noncoding random sequence, 5' ACG TTG GTC CTG CGG GAA 3', was found to assemble proticles efficiently by complexation with protamine free base (Sigma, Vienna, Austria). Protamine free base, cholesterol, and all other chemicals were purchased from Sigma in the highest available quality. Palmitoyl-oleoyl-phosphatidylcholine (POPC), polyethyleneglycol-conjugated distearyl-phosphatidylethanolamine (DSPE-PEG2000), and functionalized lipids as 1,2-distearoyl-sn-glycero-3-phosphoethanolamine-N-[maleimide (polyethylene glycol)2000] (DSPE-Mal-PEG) and 1,2-dipalmitoyl-sn-glycero-3-phosphothioethanol (DPP-TE) were purchased from Avanti Polar Lipids (Alabaster, AL). Milli-Q water was purified using a Milli-Q Plus system (Millipore, Vienna, Austria).

Recombinant mouse globular adiponectin was raised in *Escherichia coli*, and a monoclonal mouse anti-human adiponectin antibody was used as the primary antibody (Atgen, Gyeonggi-do, South Korea). An Alexa Fluor 488-prelabeled rat anti-mouse CD68 antibody was used as a macrophage marker, and nonspecific rat anti-human IgG2a was used as the negative control (AbD Serotec, Dusseldorf, Germany). As a long wavelength emitting dye, Atto655 (Atto-Tec GmbH, Siegen, Germany) was used either as a maleimide-functionalized label (Atto655-Mal) or as an amine-reactive carboxylic acid succinimidyl ester (Atto655-NHS).

Fluorescence labeling procedures

Labeling procedures for proteins and antibodies followed standard protocols recommended by the supplier of the

reactive fluorophores (see www.atto-tec.com), with slight modifications in the molar ratios of dye to protein/antibody. In the case of gAd, labeling was performed by coupling of Atto655-Mal to the single cysteine residue of the protein using a 20-fold molar excess of dye under basic conditions in phosphate-buffered saline 10 mM and 150 mM NaCl at pH 8.0. Rat anti-human IgG2a was labeled with amine-reactive Atto655-NHS, labeling the side chains of lysine residues under equimolar conditions with Atto655-NHS in 150 mM bicarbonate buffer containing 5 mM ethylenediamine tetra-acetic acid at pH 8.3. All labeling procedures were carried out at room temperature, followed by extensive dialysis at 4°C to stop the reaction and to remove nonbound dye. Dialysis was performed in microdialysis buttons (Hampton Research, Aliso Viejo, CA) using dialysis membranes with a molecular weight cutoff of 5–50 kDa, depending on the molecular mass of the labeled protein.

Phospholipid labeling was performed using a four-fold molar excess of DPP-TE dissolved in methanol over Atto655-Mal dissolved in dimethylsulfoxide. The reaction was performed in phosphate-buffered saline by incubation overnight at 37°C. The coupling reaction mixture was analyzed by high-pressure liquid chromatography (Vydac®, polymer RP column; Grace, Deerfield, IL) and purified by numerous high-pressure liquid chromatography runs. The yield was about 79%. The product was dried and stored at −20°C.

Preparation of gAd-coated stealth liposomes

Liposomes consisted of POPC/cholesterol/DSPE-PEG2000 (optionally functionalized with maleimide)/DPP-TE-Atto655 (optional dye component) at molar ratios of 3/2/0.3/0.01. Liposomes (lipid content 30 mg/mL) were made using the dry film rehydration technique as described previously.[27] gAd was thiolated with 2-iminothiolan in phosphate-buffered saline at pH 8.0 to react more efficiently with maleimide. After dialysis, 200 µg of gAd were added to preformed extruded liposomes (molar maleimide to protein ratio 30:1) in phosphate-buffered saline, at pH 8, and incubated overnight at room temperature under constant slight agitation. The reaction was stopped by adding a 10-fold molar excess of β-mercaptoethanol. Subsequently, the blocking agent and nonbound protein were removed by extensive dialysis against 10 mM phosphate-buffered saline, pH 7.4, using a dialysis membrane with a cutoff of 300 kDa. Due to the presence of fluorescence labels, the protein concentration was determined by the method of Starcher.[28] The binding efficiency of protein to lipid was about 20%. These data and estimation of the theoretical number of lipids which form one single liposome (calculations based on liposome size and surface area per phospholipid molecule) allowed a rough quantification of the number of gAd molecules per liposome. The final ratio of protein to fluorophore was 1:5 (mol/mol).

Preparation of gAd-coated proticles

Proticles comprised of oligonucleotides or Alexa-488-ON and protamine free base were prepared in aqueous solution by mixing. The composition of proticles is given as mass ratio between the components in the sequence ON:protamine, eg, 1:3 corresponding to 100 µg/mL of oligonucleotides and 300 µg/mL of protamine free base. Proticle formation occurred within the first few seconds of component incubation based on a self-assembly process, due to strong ionic interactions between oppositely charged biomolecules. Reproducibility of proticle formation was guaranteed by accurate mixing of equal volumes of the components with a pipette and vortexing for 5 seconds as described previously.[15,17] Batch sizes were used in the range of 500–1000 µL proticle suspensions. The preassembled proticles were incubated with 150 ng/10 µg oligonucleotides of native or fluorescence-labeled gAd for 1 hour at room temperature in an orbital shaker (300 rpm), and were immediately used for the subsequent staining experiments.

Radioactive labeling of gAd

To determine the binding capacity of gAd to proticles, gAd was radiolabeled with I^{125}. 500 µg gAd in phosphate-buffered saline (1 µg/µL) were mixed with 3.5 mL 170 mM bicarbonate buffer ($NaHCO_3$, pH 8.2) and concentrated using Amicon centrifugal filter devices with a cutoff of 3 kDa (Millipore, Carrigtwohill, Ireland). This step was repeated twice and the probe was finally concentrated to the start volume of 500 µL. Photometric measurement of the protein concentration at 280 nm showed a loss rate of 30%. Then the probe was labeled with 0.5 mCi of ^{125}I, vortexed, incubated with 5 µL N-bromosuccinimide (1 mg/mL), vortexed again, and incubated for 10 minutes at room temperature, as described by Sinn et al.[29] A Sephadex PD 10 column was equilibrated with 10 mM phosphate-buffered saline (pH 7.4), and the radiolabeled gAd was transferred to the column and eluted with 3.5 mL of the same buffer. To determine the free rather than adiponectin-associated radioactivity, 100 µL of adiponectin solution was centrifuged in a Microcon filtration tube at 13,000 rpm for 20 minutes (Millipore, Decatur, IL; cutoff 3 kDa). The flow through was diluted (1:1000) and counted on a Perkin Elmer Wallac Wizard 1470 automatic

gamma counter (Waltham, MA). When free radioactivity reached a value less than 5% of total radioactivity, the labeled adiponectin was used for proticle formation.

Nanocarrier characterization

The particle size (hydrodynamic diameter), broadness of size distribution (polydispersity index), and zeta potential (electrophoretic mobility) of the nanocarriers were determined using either the Malvern Zetasizer HSA3000 or the Nanosizer ZS (both from Malvern, Herrenberg, Germany). Samples were diluted with Milli-Q water and the measurements were carried out at 25°C. Formulations, including proticles consisting of oligonucleotides (or Alexa-488-ON) and protamine free base (mass ratio ON:protamine 1:3), as well as gAd-coated proticles (mass ratio ON:protamine:gAd 1:3:0.025) were investigated. Similarly, liposomes were measured as gAd-coated and noncoated formulations.

The shape and morphology of the nanoparticles were assessed by small-angle X-ray scattering or electron microscopy. Proticles, as well as gAd-coated proticles, were freeze-dried and sputtered with chromium (coating thickness approximately 9 nm) in a gas discharge apparatus (GEA005 specimen penetration energy about 10 eV) under argon atmosphere (about $8–10^{-2}$ Pa). Ultra high-resolution imaging was performed at low acceleration voltage using a Zeiss Ultra 55 field emission scanning electron microscopy with Gemini® technology (Graz University of Technology, Graz, Austria). This microscope provides a high efficiency in lens secondary electron detector for high-contrast surface imaging.

For the liposomes, transmission electron microscopic images were recorded using a Zeiss EM902 electron microscope (Oberkochen, Germany) operated at an acceleration voltage of 50 kV. Briefly, 10 µL of the liposomal suspensions were applied to a carbon-over-pioloform-coated grid and incubated for 1 minute. The excess was drawn off with filter paper and replaced immediately by 10 µL of ammonium molybdate solution (2% in phosphate-buffered saline, pH 7.4). Samples were incubated for 2 minutes, blotted, air-dried, and viewed using a magnification of 30,000×.

Qualitative proof for coupling was performed with uncoated and gAd-coated liposomes using native polyacrylamide gel electrophores is followed by Western blot analysis (data not shown) and small-angle X-ray scattering. Small-angle X-ray scattering curves were measured using a SWAX camera (System 3, Hecus X-ray Systems, Graz, Austria) mounted on a sealed X-ray tube generator from Seifert (Ahrensburg, Germany) that was operated at 50 kV and 40 mA. The X-ray beam was filtered for CuKα radiation ($\lambda = 0.1542$ nm) using a nickel foil and a pulse height discriminator. Small-angle X-ray scattering patterns were recorded using a linear, one-dimensional, position-sensitive detector (PSD 50-M, Hecus X-ray Systems, Graz, Austria). The X-ray beam size was 0.5 mm × 3.5 mm (vertical to horizontal). Calibration of the small angle region was performed with silver stearate. The samples were filled into 1 mm thick, thin-walled quartz glass capillaries, and measured for 3,600 seconds at room temperature. The background corrected scattering curves were evaluated by the GAP program[30] to determine the bilayer thickness from the corresponding electron density profiles.

The binding efficiency of gAd to preassembled proticles was evaluated with radiolabeled gAd. Three different concentrations, ie, 250, 500, and 1000 ng gAd/10 µg oligonucleotides, were incubated for 1 hour at room temperature in an orbital shaker (300 rpm). After centrifugation at 20,000 × g at 4°C for 2 hours (5804 R centrifuge; Eppendorf, Hamburg, Germany), the binding efficiency was determined by counting the gamma radiation of the supernatant and pellet separately on a Perkin Elmer Wallac Wizard 1470 automatic gamma counter.

Animal experiments

All animal procedures were approved by the Ministry of Science and Research, Austria. Apolipoprotein E-deficient mice, aged 2–4 months, with a C57BL/6J genetic background (Charles River Laboratories, Brussels, Belgium) were fed on Western-type (21% XL) experimental food (Ssniff Spezialitäten GmbH, Soest, Germany) for 2–3 months. At least three mice were used for each staining trial. Age-matched C57BL/6J wild type mice (Medical University of Vienna, Austria) were used as the control strain. Due to the fact that these mice developed no atherosclerotic lesions, just one mouse was used as a negative control per staining trial. All experiments were performed independent of gender. Injured endothelium was defined as the activated endothelial layer covering the atherosclerotic lesions of apolipoprotein E-deficient mice. For each ex vivo staining trial, the mice were sacrificed randomly with an overdose of isoflurane (Abbott GmbH, Vienna, Austria). The chest was opened, the circulation was rinsed immediately with phosphate-buffered saline (pH 7.4) for 15 minutes by perfusing the heart using an injection needle, and the vena cava was transected. The aorta, including the aortic arch, was dissected, cut open, washed with phosphate-buffered saline (pH 7.4), and incubated in Krebs–Henseleit solution (118 mM NaCl; 25 mM

$NaHCO_3$; 2.8 mM $CaCl_2$ 2 H_2O; 1,17 mM $MgSO_4$ 7 H_2O; 4,7 mM KCl; 1,2 mM KH_2PO_4; 2 mg/mL glucose; pH 7.4) to sustain its physiological activity while blocking nonspecific binding reactions with 1% bovine serum albumin (Sigma) for 1 hour at room temperature. The samples were then incubated with the fluorescence-labeled biomarker (20 µg/mL of Atto655-labeled gAd), antibodies (nonspecific rat anti-human IgG2a, or 5 µg/mL of AF488-labeled anti-CD68 for positive control) or gAd-coated nanoparticles (2 mg/mL Atto655-labeled gAd-coated stealth liposomes, Atto655-labeled stealth liposomes for negative control; 100 µg/mL AF488-labeled gAd-coated proticles or AF488-labeled gAd-Atto655-coated proticles and AF488-labeled proticles for negative control) for 1–2 hours at 37°C with shaking in the dark to avoid fluorochrome bleaching. Hoechst 33342 fluorescence dye (1 µg/mL, Invitrogen, Carlsbad, CA) was added to stain the cell nuclei. Subsequently, the aortic sections were washed 3–4 times in phosphate-buffered saline (pH 7.4), put on a glass slide, covered with polyvinyl alcohol mounting medium containing 1,4-diazabicyclo[2.2.2]octane (DABCO, Sigma), adjusted under a stereomicroscope, and overlaid with a cover slip.

Fluorescence imaging by confocal laser scanning microscopy

All fluorescence and transmitted light images of the aortic samples (Z-stack images) were acquired with the LSM 510 Meta Axiovert 200M Zeiss confocal system (Jena, Germany). Images were collected using a 40 × Plan-Neofluar 1.3 DIC oil immersion objective and a multitrack configuration, with which the Hoechst Alexa Fluor 488 and Atto655 signals were sequentially collected with BP 420–480 nm, BP 50–550 nm, and BP 679–743 nm filters after excitation with 405, 488, and 633 nm laser lines, respectively. In the sequential acquisitions for all three channels, the Zeiss AIM software (v 4.2) was used. All confocal images were acquired with a frame size of 1024 × 1024 pixels averaged three times.

Results

Physicochemical characterization of gAd-coated nanoparticles

Proticles (mass ratio ON:protamine 1:3) showed a mean particle diameter of about 188 nm for uncoated and 263 nm for gAd-coated proticles (mass ratio ON:protamine:gAd 1:3:0.025). An adequate size distribution with polydispersity values between 0.03 and 0.30, and zeta potential values of 28.1 ± 3.9 mV for uncoated proticles and 16.7 ± 2.6 mV for gAd-coated proticles were recorded. For liposomes, the average particle diameter increased upon gAd coupling from about 100 nm (polydispersity index approximately 0.04) to about 160 nm (polydispersity index approximately 0.18), with zeta potentials decreasing from –9.4 ± 1.3 mV to –21.9 ± 1.2 mV. All data are summarized in Table 1.

Transmission electron microscopic images of liposomes showed spherical particles (Figure 1A), the integrity of which was preserved after ligand coupling, as indicated by the small-angle X-ray scattering data, which give an impression of bilayer thickness and organization. The scattering contribution of ligands coupled onto the surfaces of the liposomes is seen in the scattering profiles (Figure 1B). However, the bilayer lamellarity and thickness (d = approximately 3.6 nm) was not impaired by the ligand-coupling procedures. By analogy, the scanning electron microscopic images of the freeze-dried proticle suspensions showed single, mostly spherical adiponectin-coated proticles (Figure 1C). Determination of binding efficiency using I^{125}-labeled gAd showed a maximum coupling efficiency of approximately 150 ng gAd/10 µg oligonucleotides (Figure 1D).

Table 1 Nanoparticle size, polydispersity index, and zeta potential of unloaded and gAd-coated nanoparticles. The nanoparticle size (hydrodynamic diameter), polydispersity index, and zeta potential of two different preparations were determined using photon correlation spectroscopy. In this study, unloaded proticles (ON:protamine 1:3), gAd-coated proticles (ON:protamine:gAd 1:3:0.025) as well as plain or gAd-coated liposomes were characterized concerning these parameters. Results express mean values ± standard deviations from six measurements for each preparation

Samples	Mass ratio	Hydrodynamic diameter (nm)	Polydispersity index	Zeta potential (mV)	pH value
ON/protamine	1:3	188.1 ± 13.2	0.03 ± 0.02	28.1 ± 3.9	9.36 ± 0.20
ON/protamine/gAd	1:3:0.025	263.1 ± 27.2	0.30 ± 0.09	16.7 ± 2.6	9.18 ± 0.09
POPC/DSPE-PEG2000/ cholesterol		98.4 ± 6.5 (n = 8)	0.04 ± 0.02	–9.4 ± 1.3	7.4
POPC/DSPE-PEG2000-mal-gAd/cholesterol	20:1 (lipid to protein)	165 ± 13.5 (n = 4)	0.11 ± 0.05	–21.9 ± 1.2	7.4

Abbreviations: ON, oligonucleotides; gAd, globular domain of the adipocytokine adiponectin; POPC, palmitoyl-oleoyl-phosphatidylcholine; DSPE-PEG2000, polyethylene glycol conjugated distearyl-phosphatidylethanolamine.

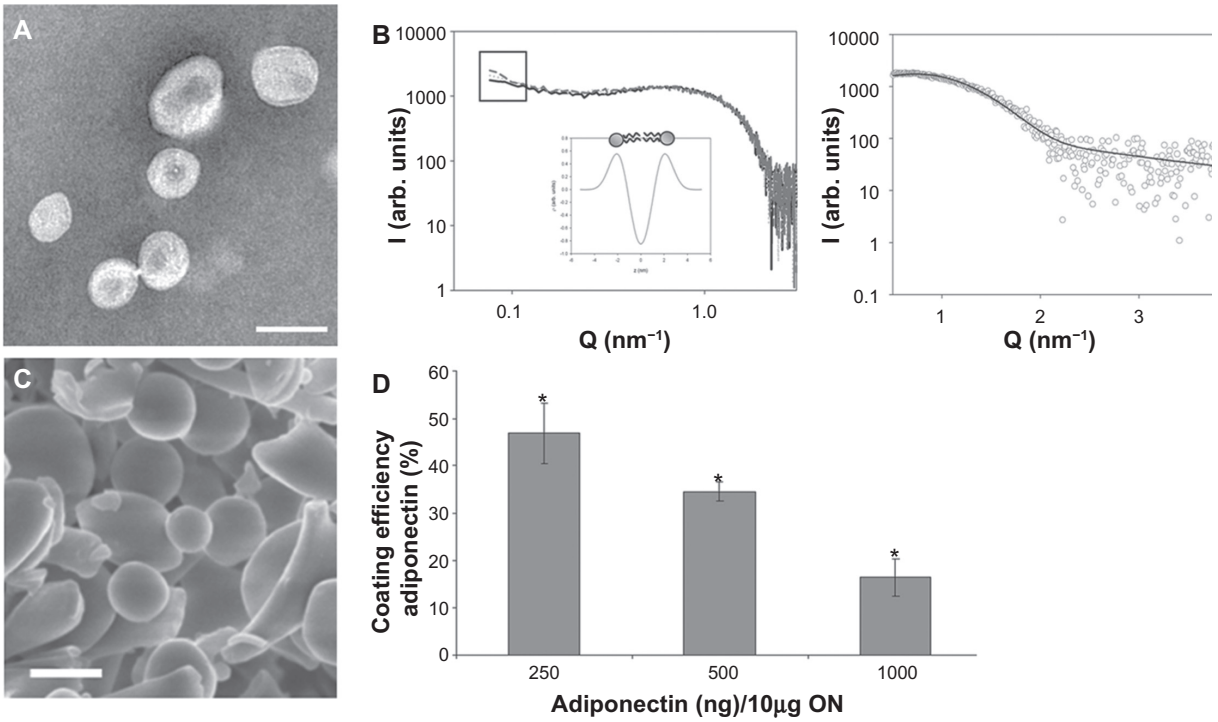

Figure 1 Characterization of gAd-coated nanoparticles. **A**) Liposomes. A representative transmission electron microscopy image (white bar indicates 100 nm) highlights the size distribution and morphology of liposomes. **B**) Small angle X-ray scattering of uncoated and gAd-coated liposomes. The intrinsic lipid bilayer parameter (eg, lamellarity and thickness) derived from SAXS curves were not affected by ligand coupling (uncoated liposome [black line], fluorescent-labeled liposome [dotted line] and gAd-coupled liposome [dashed line]). The contribution of dye/protein to the scattering intensity is seen at a low q-range (marked by a frame). The best fit to the data obtained from deconvolution is shown on the right side. The calculated electron density profile, that allows for the determination of the bilayer thickness, estimated as phospholipid head-to-head group distance, d, is shown as an inset on the left side. **C**) Proticles. Scanning electron microscopy images of freeze-dried adiponectin-coated proticles (mass ratio ON:protamine:adiponectin 1:3:0.025; white bar indicates 250 nm). **D**) Coating efficiency of adiponectin to proticles. Preassembled proticles were incubated with various amounts of radiolabeled gAd. Calculation of coating efficiency as percentage of deployed adiponectin showed a constant binding amount of gAd to oligonucleotides (analysis of variance, $P < 0.05$, n = 3).

Abbreviations: gAd, globular domain of adiponectin; ON, oligonucleotides.

Staining of atherosclerotic plaques with gAd-coated stealth liposomes

The aortas were incubated with Atto655-labeled stealth liposomes because no interfering autofluorescence signal was observed at $\lambda_{ext} = 633$ nm for unstained blank sections, neither from the whole uninjured aortic tissue nor from the scanned atherosclerotic plaques (Figure 2A). We found a dotted fluorescence signal pattern on the aortic sections of apolipoprotein E-deficient mice, particularly in the plaque regions and in the less injured surrounding area (Figure 2B). Sections from wild type mice were stained as controls, showing only weak signals at the generally uninjured aortic surface. A similar low staining pattern was observed for gAd-coated stealth liposomes on the uninjured sections from wildtype mice and at less injured aortic sections of apolipoprotein E-deficient mice. In contrast, a strong signal was detected from the gAd-coated stealth liposomes at atherosclerotic plaque areas (Figure 2C). The staining signal of gAd-coated liposome partially colocalizes with CD68-stained monocytes/macrophages, which were detected at the plaque surface (Figure 3).

Staining of atherosclerotic plaques with gAd-coated proticles

Next, we examined the staining features of the proticles. Sections from the inner aortic surface of apolipoprotein E-deficient and C57Bl6/J wild type mice were imaged by confocal laser scanning microscopy, unstained or stained with either AF488-labeled proticles or gAd-coated AF488-labeled proticles. Unstained blank sections showed a weak autofluorescence signal at $\lambda_{ext} = 488$ nm detected from the whole uninjured aortic tissue. In the specific atherosclerotic plaque area, only a small portion of fluorescence emitting inclusions were observed, whereas neither the plaques nor the plaque surface showed obvious interference caused by the autofluorescence signal of the tissue (Figure 4A). To examine the nonspecific binding of proticles to aortic tissue, we incubated aortic sections from apolipoprotein E-deficient and wildtype mice with AF488-labeled proticles. We observed a weak staining signal on the whole aortic surface. However, on atherosclerotic plaque areas, we saw a stronger spotted fluorescence signal pattern (Figure 4B). Using CD68 staining, we

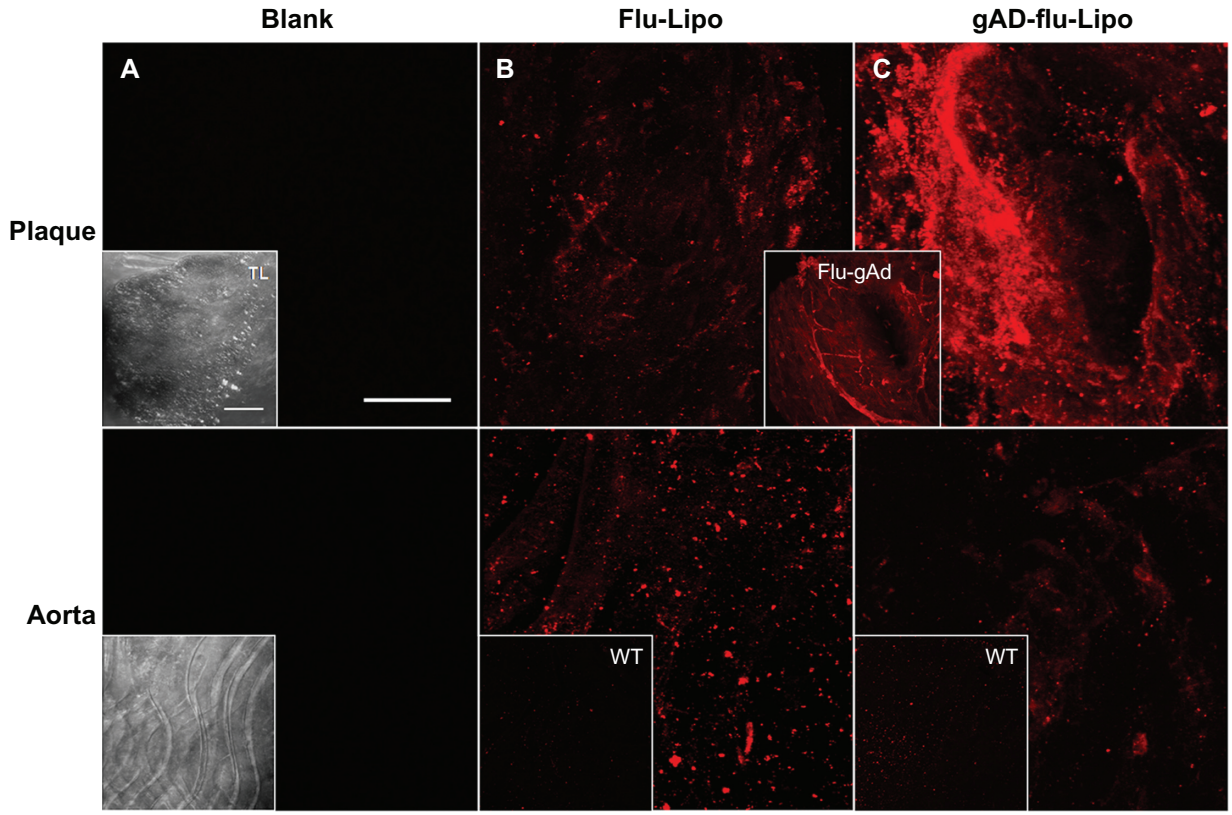

Figure 2 The staining signal of liposomal nanoparticles at atherosclerotic plaques is enhanced by globular adiponectin. Aortic sections of apolipoprotein E-deficient and C57Bl6/J wild type mice were incubated with Atto655-labeled stealth liposomes as controls (**B**), or with gAd-coupled Atto655-labeled liposomes (**C**). Blank sections are shown in (**A**). The upper panels correspond to plaque regions, while the lower panels show the signals in artery sections without plaques. The inserts (**B**, **C**) show the weak fluorescence signals from stained wild type aortic tissue. Transmitted light images of the aortic sections are shown in (**A**) (inserts). The insert between (**B**) and (**C**) displays the accumulation of Atto655-labeled gAd at atherosclerotic plaques for comparison. Sections were placed between a glass slide and a cover slip and visualized by confocal laser scanning microscopy (fluorescence and transmitted light). For each visualization, a series of 20–30 fluorescence images in Z (1 μm consecutive intervals) were projected in a single image. Both bars indicate 50 μm.
Abbreviation: gAd, globular domain of adiponectin.

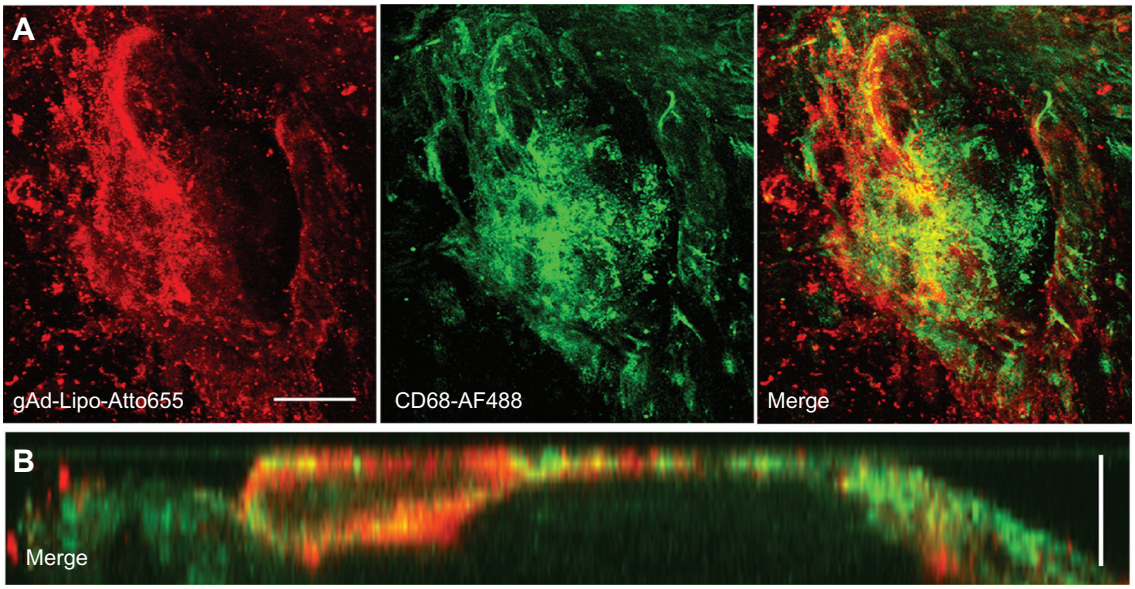

Figure 3 Costaining for anti-CD68. Aortic sections of apolipoprotein E-deficient mice were incubated with Atto655-labeled gAd-coupled stealth liposomes and costained with an Alexa Fluor 488 ready-labeled mouse anti-CD68 antibody. **A**) Three-dimensional fluorescence images from an atherosclerotic plaque. Bar indicates 50 μm. **B**) Vertical fluorescence image of the same plaque. Vertical bar indicates 15 μm. The yellow signal in the merged images indicates the colocalization of gAd liposomes (red signal) and anti-CD68 (green signal).
Abbreviation: gAd, globular domain of adiponectin.

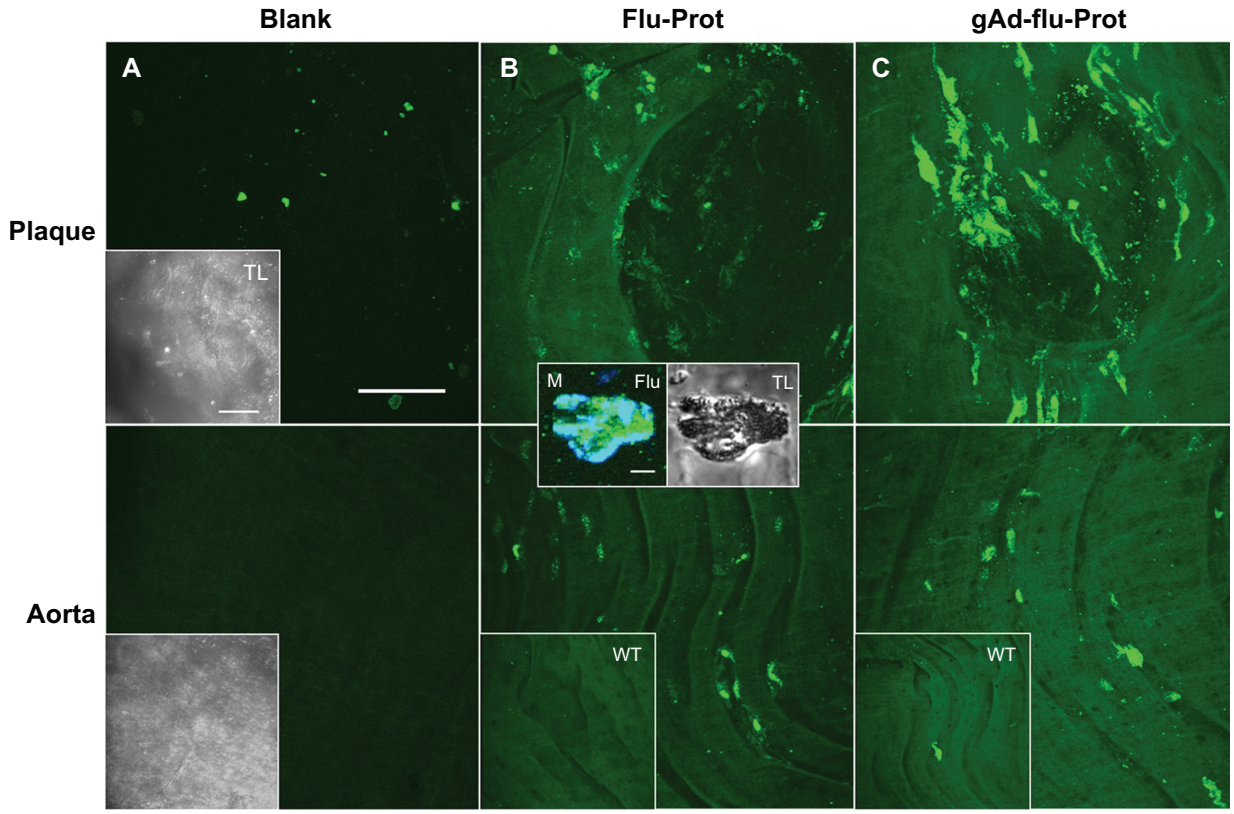

Figure 4 The staining signal of globular adiponectin at atherosclerotic plaques is altered by protamine-oligonucleotide-based nanoparticles. Aortic sections of apolipoprotein E-deficient and C57Bl6/J wild type mice were incubated with Alexa Fluor 488-labeled proticles for control (**B**), or with gAd-coupled, Alexa Fluor 488-labeled proticles (**C**). Blank sections are shown in (**A**). The upper panels correspond to plaque regions, while the lower panels show the signals in artery sections without plaques. The inserts (**B**, **C**) show the weak fluorescence signals from stained wild type aortas. Transmitted light images of the aortic sections are shown in (**A**) (inserts). The inserts in (**B**) show the accumulation of proticles (green signal) inside a CD68-verified macrophage (M, blue signal). Both bars in (**A**) indicate 50 μm, bar in the first insert in (**B**) indicates 5 μm.
Abbreviation: gAd, globular domain of adiponectin.

found a colocalization of the fluorescence signals (Figure 4, middle panel), which is indicative of internalization of the proticles, most likely by macrophages. To investigate the selective targeting ability of the proticles, aortic sections were incubated with gAd-coated proticles. In the confocal laser scanning microscopy images, we observed strong enhancement of the fluorescence signal, still showing the spotted fluorescence pattern observed for nontargeted proticles (Figure 4C).

Signal enhancement by gAd-targeted nanoparticles in comparison with free gAd

gAd-coated liposomes behaved in a manner similar to that of free Atto655-labeled gAd (flu-gAd), because they did not penetrate into the atherosclerotic plaque, but accumulated at the plaque surface, and thereby produced a pronounced increase in signal intensity when compared with flu-gAd (Figures 5A and 5B).

Flu-gAd coupled with Alexa Fluor 488-labeled proticles showed a considerably altered staining pattern in the plaque scenario as compared with free uncoupled flu-gAd. As already mentioned above, the staining pattern changed to a spotted macrophage-specific staining, which was markedly amplified compared with that of the uncoated proticles. Most interestingly, gAd-coated proticles penetrated the plaque deeper than did free flu-gAd (Figure 5C). As a negative control, aortic sections from apolipoprotein E-deficient mice were stained with Atto655-labeled nonspecific rat IgG. Only traces of unspecific IgG accumulation on the atherosclerotic plaques were detected (Figure 6).

Discussion

Drug delivery and noninvasive imaging applications with the help of targeted nanoparticles are becoming more and more important in modern medicine.[31,32] Beyond this, nanoparticles offer new possibilities as homing devices for various drugs or contrast agents. Although cancer therapy and cancer

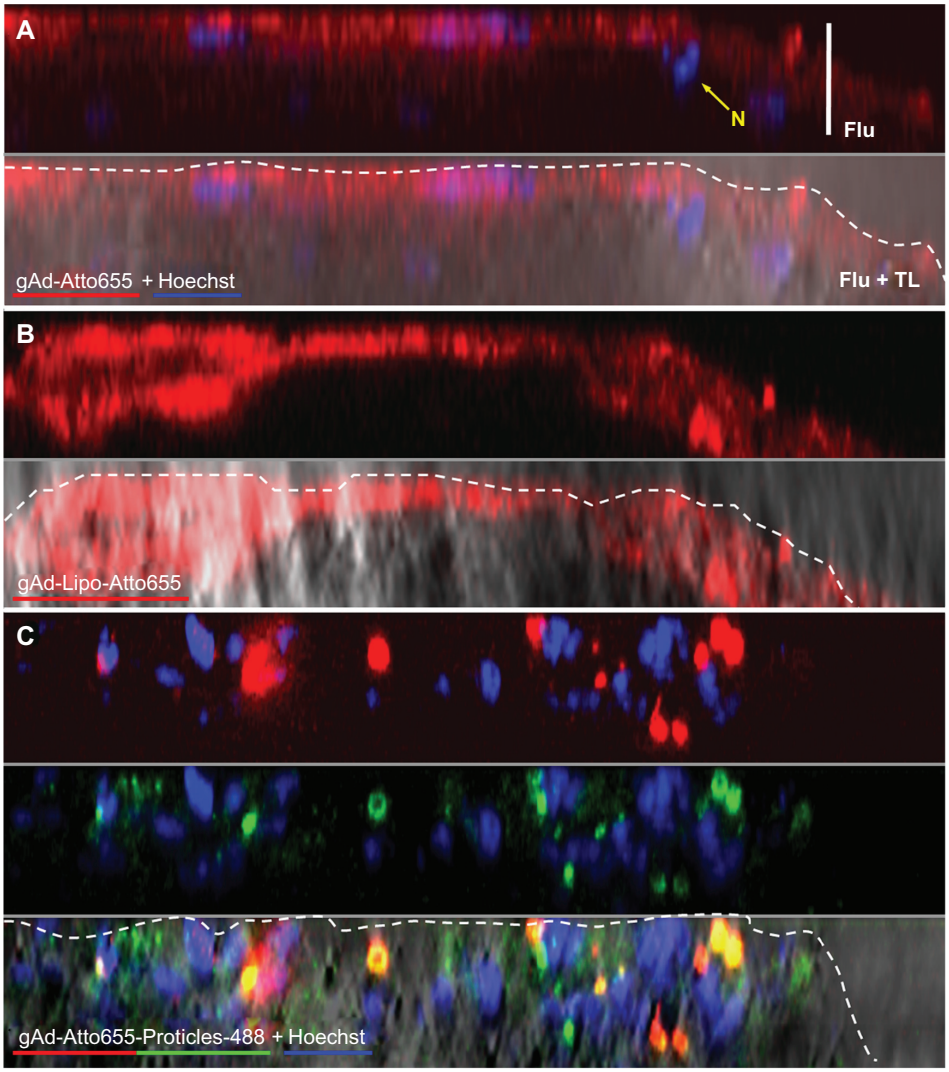

Figure 5 Plaque imaging of gAd-coupled nanoparticles in comparison with uncoupled gAd. Aortic sections of apolipoprotein E-deficient mice were incubated with (**A**) Atto655-labeled gAd, (**B**) gAd-coupled Atto655-labeled liposomes, or (**C**) Atto65-labeled gAd coupled to Alexa Fluor 488-labeled proticles. The pictures show vertical fluorescence and transmitted light images from atherosclerotic plaques similar in size. Nuclei were costained with Hoechst nucleus dye. The yellow signal in the merged image in (**C**) indicates the colocalization of gAd (red signal) and proticles (green signal). The dashed white lines mark the boundary layer of the plaques. Vertical bar indicates 15 µm.
Abbreviation: gAd, globular domain of adiponectin.

diagnostics are still dominating the field, the detection of atherosclerotic plaques is an equally attractive endeavor in the prevention of cardiovascular diseases.[33,35] Atherosclerosis is a chronic disease in which inflammatory processes are the driving forces for the formation, progression, and rupture of atherosclerotic plaques.[36] One key event in atherosclerosis is the differentiation of monocytes into lesional macrophages, a process driven by inflammatory cascades.[37] Consequently, several mediators involved in the inflammatory process during the progression of atherosclerosis have been suggested as potential biomarkers to recognize atherosclerotic lesions.[34] In addition, adipocytokines, such as adiponectin, are suggested as promising candidates.[38]

In the present study, we chose the globular domain of adiponectin as a targeting sequence, because we had already shown that free gAd detects atherosclerotic lesions very well (unpublished data). We found that gAd accumulated in the endothelial cells and fibrous cap area of atherosclerotic plaques. Here we address the question of whether signal enhancement, which is necessary for high-resolution detection in vivo, can be achieved when gAd is coupled with nanoparticles serving as transporters of signal-emitting molecules. Specifically, we have tested two different kinds of nanoparticles, namely stealth liposomes and proticles, and used an apolipoprotein E-deficient mouse model fed on a Western-type diet as a model system for atherosclerosis.

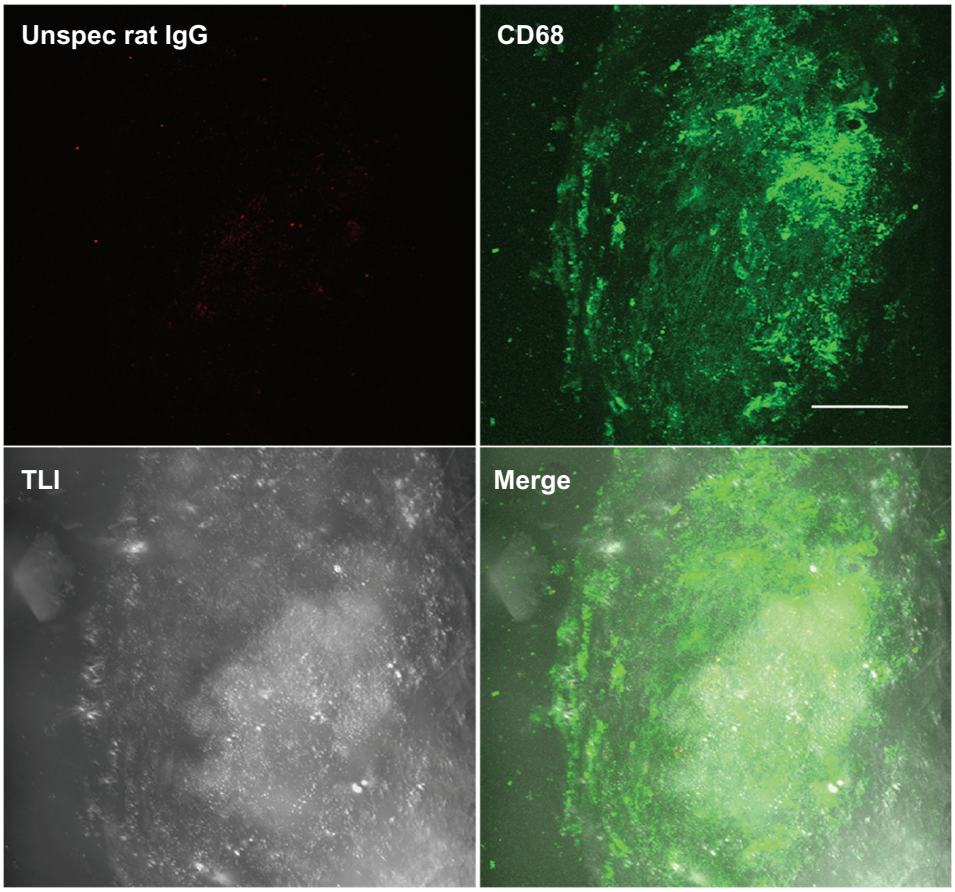

Figure 6 Negative control staining. Three-dimensional fluorescence and transmitted light images from an atherosclerotic plaque. Aortic sections of apolipoprotein E-deficient mice were stained with Atto655-labeled unspecific rat IgG and costained with Alexa Fluor488 ready-labeled mouse anti-CD68. Bar indicates 50 μm.

Liposomes are one of the most widely studied classes of nanoparticles. They are composed of biologically degradable phospholipid molecules, and in aqueous solution they typically assemble to form closed bilayer structures.[39] They are easy to handle, and offer a unique variety of combination possibilities because of their overall size and charge. Surface coating with polymers like polyethylene glycol significantly enhances their circulation time because they are not rapidly cleared by the reticular endothelial system.[23] Likewise, functionalized groups can be attached to the distal end of the polyethylene glycol chains for coupling of active molecules.[40] Alternatively, different labels can be linked to or incorporated into the liposomes.[41,42]

Proticles are less well explored, but have already proven to be very successful in drug targeting. They can be coated with targeting ligands, such as small peptides, and also with larger proteins like apolipoprotein A-1.[18] In an earlier study, we demonstrated improved permeability of the blood–brain barrier for proticles with apolipoprotein coating. Recently, we investigated the targeting effect of vasoactive intestinal peptide, which was incorporated into the proticle matrix. Using this system, we could demonstrate a targeted association of proticles on the cell surface in vitro and a specific localization of proticles into vasoactive intestinal peptide receptor-positive lung tumor material ex vivo.[43]

In the present study, both kinds of nanoparticles were coated with the same targeting sequence, either by covalent attachment of gAd to the polyethylene glycol spacer on the surface of liposomes or electrostatically bound to the surface of the proticles. A comparably high amount of gAd was attached to the nanocarriers, corresponding to about 15 ng gAd per μg of oligonucleotides or, on average, 65 thiolized gAd molecules per liposome. Whereas the size of the liposomes was kept below 200 nm with a negative zeta-potential, proticles were somewhat larger and had a positive net surface charge.

To study the potential for molecular imaging, we have performed confocal laser scan fluorescence microscopy to evaluate the efficiency of the targeted nanocarriers to recognize atherosclerotic plaques ex vivo. Both classes of gAd-targeted nanoparticles led to remarkable signal enhancement compared with free gAd, while untargeted

proticles showed fewer untargeted liposomes, and had almost no binding affinity for atherosclerotic plaques. The most striking feature of our study was that the two classes of targeted nanoparticles demonstrated distinct differences in their binding/internalization behavior, strongly depending on the nature of the nanocarrier.

Apart from chemical composition, particle size, and morphology, surface charge is an important parameter influencing interactions and uptake of macromolecules.[44] In general, the phagocytic activity of macrophages is higher for anionic than for cationic nanoparticles.[45,46] Neutral nanoparticles showed the lowest uptake, at least in vitro.[47,48] In our study, we used positively charged proticles and slightly negatively charged liposomes. After gAd (isoelectric point 5.4) coupling, the surface net charge was further decreased. Hence, the observed differences in the interaction mechanisms of nanoparticles with the plaque could well be charge-dependent. However, negatively charged, sterically stabilized gAd-coated liposomes accumulated at the outer surface of the plaque, similar to free flu-gAd, and generated a strong signal enhancement at the plaque surface, ie, the so-called fibrous cap area. The targeted liposomes colocalized with monocytes/macrophages detected in this region by anti-CD68 costaining. Positively charged proticles adhered more tightly to the arterial wall of atherosclerotic plaques, probably due to the enhanced permeability caused by the loss of the endothelial glycocalyx,[49] and were readily taken up by macrophages as proven by anti-CD68 costaining. This observed uptake by surface monocytes/macrophages and subsequent internalization in intraplaque macrophages, which represent most of the macrophages in atherosclerotic lesions, was markedly enhanced by gAd targeting. In apolipoprotein A–/– mice, mainly $Gr1^{+}/Ly6C^{hi}$ monocytes occur.[50] These monocytes were reported to adhere to activated endothelium, infiltrate lesions, and become atherosclerotic macrophages.[51] Hence, the gAd-targeted proticles could be a useful device for further cell tracking experiments and exploring the progression of inflammation in atherosclerosis, while gAd-targeted liposomes represent promising markers for imaging of the fibrous cap.

Conclusion

Our results demonstrate the potential of gAd-targeted nanoparticles to recognize atherosclerotic lesions in the arterial wall. The approach taken here could offer, beyond diagnostic purposes, therapeutic drug targeting options for the future. However, using one specific biomarker coupled to diverse nanoparticles creates different imaging characteristics. This, in turn, offers the possibility to probe different regions within the same plaque scenario. At this point, it appears that a rational combination of diverse nanoparticles could be advantageous for the evaluation of novel targeting sequences to image inflammatory sites or even to discriminate between stable and vulnerable plaques.

Acknowledgment

This work was supported by the Austrian Nano-Initiative, which cofinanced this work as part of the Nano-Health Project, financed by the Austrian Research Promotion Agency.

Disclosure

The authors report no conflicts of interest in this work.

References

1. Havel PJ. Control of energy homeostasis and insulin action by adipocyte hormones: Leptin, acylation stimulating protein, and adiponectin. *Curr Opin Lipidol*. 2002;13(1):51–59.
2. Shimada K, Miyazaki T, Daida H. Adiponectin and atherosclerotic disease. *Clin Chim Acta*. 2004;344(1–2):1–12.
3. Kadowaki T, Yamauchi T. Adiponectin and adiponectin receptors. *Endocr Rev*. 2005;26(3):439–451.
4. Hug C, Lodish HF. The role of the adipocyte hormone adiponectin in cardiovascular disease. *Curr Opin Pharmacol*. 2005;5(2):129–134.
5. Fang X, Sweeney G. Mechanisms regulating energy metabolism by adiponectin in obesity and diabetes. *Biochem Soc Trans*. 2006;34(Pt 5):798–801.
6. Fruebis J, Tsao TS, Javorschi S, et al. Proteolytic cleavage product of 30-kDa adipocyte complement-related protein increases fatty acid oxidation in muscle and causes weight loss in mice. *Proc Natl Acad Sci U S A*. 2001;98(4):2005–2010.
7. Bruce CR, Mertz VA, Heigenhauser GJ, Dyck DJ. The stimulatory effect of globular adiponectin on insulin-stimulated glucose uptake and fatty acid oxidation is impaired in skeletal muscle from obese subjects. *Diabetes*. 2005;54(11):3154–3160.
8. Palanivel R, Fang X, Park M, et al. Globular and full-length forms of adiponectin mediate specific changes in glucose and fatty acid uptake and metabolism in cardiomyocytes. *Cardiovasc Res*. 2007;75(1):148–157.
9. Yamauchi T, Kamon J, Waki H, et al. Globular adiponectin protected ob/ob mice from diabetes and ApoE-deficient mice from atherosclerosis. *J Biol Chem*. 2003;278(4):2461–2468.
10. Chen H, Montagnani M, Funahashi T, Shimomura I, Quon MJ. Adiponectin stimulates production of nitric oxide in vascular endothelial cells. *J Biol Chem*. 2003;278(45):45021–45026.
11. Li CJ, Sun HW, Zhu FL, et al. Local adiponectin treatment reduces atherosclerotic plaque size in rabbits. *J Endocrinol*. 2007;193(1):137–145.
12. Okamoto Y, Arita Y, Nishida M, et al. An adipocyte-derived plasma protein, adiponectin, adheres to injured vascular walls. *Horm Metab Res*. 2000;32(2):47–50.
13. Ouchi N, Kihara S, Arita Y, et al. Adipocyte-derived plasma protein, adiponectin, suppresses lipid accumulation and class A scavenger receptor expression in human monocyte-derived macrophages. *Circulation*. 2001;103(8):1057–1063.
14. Junghans M, Kreuter J, Zimmer A. Antisense delivery using protamine-oligonucleotide particles. *Nucleic Acids Res*. 2000;28(10):E45.
15. Lochmann D, Weyermann J, Georgens C, Prassl R, Zimmer A. Albumin-protamine-oligonucleotide nanoparticles as a new antisense delivery system. Part 1: Physicochemical characterization. *Eur J Pharm Biopharm*. 2005;59(3):419–429.

16. Weyermann J, Lochmann D, Georgens C, Zimmer A. Albumin-protamine-oligonucleotide-nanoparticles as a new antisense delivery system. Part 2: Cellular uptake and effect. *Eur J Pharm Biopharm*. 2005;59(3):431–438.
17. Wernig K, Griesbacher M, Andreae F, et al. Depot formulation of vasoactive intestinal peptide by protamine-based biodegradable nanoparticles. *J Control Release*. 2008;130(2):192–198.
18. Kratzer I, Wernig K, Panzenboeck U, et al. Apolipoprotein A-I coating of protamine-oligonucleotide nanoparticles increases particle uptake and transcytosis in an in vitro model of the blood-brain barrier. *J Control Release*. 2007;117(3):301–311.
19. Kerkmann M, Lochmann D, Weyermann J, et al. Immunostimulatory properties of CpG-oligonucleotides are enhanced by the use of protamine nanoparticles. *Oligonucleotides*. 2006;16(4):313–322.
20. Briley-Saebo KC, Mulder WJ, Mani V, et al. Magnetic resonance imaging of vulnerable atherosclerotic plaques: Current imaging strategies and molecular imaging probes. *J Magn Reson Imaging*. 2007;26(3):460–479.
21. Erdogan S. Liposomal nanocarriers for tumor imaging. *J Biomed Nanotechnol*. 2009;5(2):141–150.
22. Cormode DP, Skajaa T, Fayad ZA, Mulder WJ. Nanotechnology in medical imaging: Probe design and applications. *Arterioscler Thromb Vasc Biol*. 2009;29(7):992–1000.
23. Immordino ML, Dosio F, Cattel L. Stealth liposomes: Review of the basic science, rationale, and clinical applications, existing and potential. *Int J Nanomedicine*. 2006;1(3):297–315.
24. Samad A, Sultana Y, Aqil M. Liposomal drug delivery systems: An update review. *Curr Drug Deliv*. 2007;4(4):297–305.
25. Harding JA, Engbers CM, Newman MS, Goldstein NI, Zalipsky S. Immunogenicity and pharmacokinetic attributes of poly(ethylene glycol)-grafted immunoliposomes. *Biochim Biophys Acta*. 1997;1327(2):181–192.
26. Woodle MC. Controlling liposome blood clearance by surface-grafted polymers. *Adv Drug Deliv Rev*. 1998;32(1–2):139–152.
27. Stark B, Debbage P, Andreae F, Mosgoeller W, Prassl R. Association of vasoactive intestinal peptide with polymer-grafted liposomes: Structural aspects for pulmonary delivery. *Biochim Biophys Acta*. 2007;1768(3):705–714.
28. Starcher B. A ninhydrin-based assay to quantitate the total protein content of tissue samples. *Anal Biochem*. 2001;292(1):125–129.
29. Sinn HJ, Schrenk HH, Friedrich EA, Via DP, Dresel HA. Radioiodination of proteins and lipoproteins using N-bromosuccinimide as oxidizing agent. *Anal Biochem*. 1988;170(1):186–192.
30. Pabst G. Global properties of biomimetic membranes: Perspectives on molecular features. *Biophys Rev Lett*. 2006;1(1):57–84.
31. Wickline SA, Neubauer AM, Winter PM, Caruthers SD, Lanza GM. Molecular imaging and therapy of atherosclerosis with targeted nanoparticles. *J Magn Reson Imaging*. 2007;25(4):667–680.
32. Choudhury RP, Fisher EA. Molecular imaging in atherosclerosis, thrombosis, and vascular inflammation. *Arterioscler Thromb Vasc Biol*. 2009;29(7):983–991.
33. Sanz J, Fayad ZA. Imaging of atherosclerotic cardiovascular disease. *Nature*. 2008;451(7181):953–957.
34. Lindsay AC, Choudhury RP. Form to function: Current and future roles for atherosclerosis imaging in drug development. *Nat Rev Drug Discov*. 2008;7(6):517–529.
35. Nahrendorf M, Sosnovik DE, Weissleder R. MR-optical imaging of cardiovascular molecular targets. *Basic Res Cardiol*. 2008;103(2):87–94.
36. Libby P, Okamoto Y, Rocha VZ, Folco E. Inflammation in atherosclerosis: Transition from theory to practice. *Circ J*. 2010;74(2):213–220.
37. Woollard KJ, Geissmann F. Monocytes in atherosclerosis: Subsets and functions. *Nat Rev Cardiol*. 2010;7(2):77–86.
38. Mangge H, Almer G, Truschnig-Wilders M, Schmidt A, Gasser R, Fuchs D. Inflammation, adiponectin, obesity and cardiovascular risk. *Curr Med Chem*. 2010;17(36):4511–4520.
39. Sessa G, Weissmann G. Phospholipid spherules (liposomes) as a model for biological membranes. *J Lipid Res*. 1968;9(3):310–318.
40. Maruyama K, Takizawa T, Yuda T, Kennel SJ, Huang L, Iwatsuru M. Targetability of novel immunoliposomes modified with amphipathic poly(ethylene glycol)s conjugated at their distal terminals to monoclonal antibodies. *Biochim Biophys Acta*. 1995;1234(1):74–80.
41. Uppal R, Caravan P. Targeted probes for cardiovascular MR Imaging. *Future Med Chem*. 1;2(3):451–470.
42. Voinea M, Simionescu M. Designing of 'intelligent' liposomes for efficient delivery of drugs. *J Cell Mol Med*. 2002;6(4):465–474.
43. Ortner A, Wernig K, Kaisler R, et al. VPAC receptor mediated tumor cell targeting by protamine based nanoparticles. *J Drug Target*. 2010;18(6):457–467.
44. Parker JC. Transport and distribution of charged macromolecules in lungs. *Adv Microcirc*. 1987(13):150–159.
45. Chono S, Tauchi Y, Morimoto K. Influence of particle size on the distributions of liposomes to atherosclerotic lesions in mice. *Drug Dev Ind Pharm*. 2006;32(1):125–135.
46. Maiseyeu A, Mihai G, Kampfrath T, et al. Gadolinium-containing phosphatidylserine liposomes for molecular imaging of atherosclerosis. *J Lipid Res*. 2009;50(11):2157–2163.
47. Ahsan F, Rivas IP, Khan MA, Torres Suarez AI. Targeting to macrophages: Role of physicochemical properties of particulate carriers – liposomes and microspheres – on the phagocytosis by macrophages. *J Control Release*. 2002;79(1–3):29–40.
48. Roser M, Fischer D, Kissel T. Surface-modified biodegradable albumin nano- and microspheres. II: Effect of surface charges on in vitro phagocytosis and biodistribution in rats. *Eur J Pharm Biopharm*. 1998;46(3):255–263.
49. Nieuwdorp M, Meuwese MC, Vink H, Hoekstra JB, Kastelein JJ, Stroes ES. The endothelial glycocalyx: A potential barrier between health and vascular disease. *Curr Opin Lipidol*. 2005;16(5):507–511.
50. Plump AS, Breslow JL. Apolipoprotein E and the apolipoprotein E-deficient mouse. *Annu Rev Nutr*. 1995;15:495–518.
51. Swirski FK, Libby P, Aikawa E, et al. Ly-6Chi monocytes dominate hypercholesterolemia-associated monocytosis and give rise to macrophages in atheromata. *J Clin Invest*. 2007;117(1):195–205.